Healthcare Analytics 4 (2023) 100251

Contents lists available at ScienceDirect

Healthcare Analytics

journal homepage: www.elsevier.com/locate/health

A Hybrid Generative Adversarial network with Quantum U-NET for 3D spine X-ray image registration

Srinivasa Rao Gadu *, Chandra sekhar potala

GITAM School of Technology, GITAM Deemed to be University

ARTICLE INFO

Handling editor: Madijd Tavana

Keywords:
Image registration
Spine x-ray
Synthetic data
Generative adversarial network
Unet
Quantum neural network

ABSTRACT

The registration of Two Dimensional (2D) to Three Dimensional (3D) spine x-ray image is essential in medical field for the diagnosis of scoliosis. In the surgerical procedure of scoliosis, Computed tomography (CT) imagery and intraoperative projective X-rays are used with the requirement of implant localization. The 3D reconstruction is challenged with the presence of implant projection which affects the registration capture range. In this paper, the novel inpainting algorithm Generative Adversarial Network with Quantum Unet (GAN-Q-Unet) model is developed to resolve the issues of registration capture range. The generator network learns to produce data with the output of discriminator network. In GAN-Q-Unet, the discriminator network is replaced with the encoder-decoder network namely U-net which improves the quality of the network by providing more semantic information. In addition to that, the layers of U-net are replaced with quantum layers in which encoding and transformation is applied based on non-linearity. Initially, the bone regions of the spine image are enhanced with synthetic data generation. After enhancement, the proposed inpainting is applied for 3D image registration. With GAN-Q-Unet approach, better 3D reconstruction of spine image is obtained from 2D spine image. The proposed algorithm is used for automatic transformation of spine image with varying dimensions in the routine examination of clinical applications. By using the proposed approach, the Peak Signal to Noise Ratio (PSNR), Structural Similarity index Measure (SSIM), Dice Similarity coefficient (DSC) and Loss values obtained are 28.1767, 0.9300, 2.9674, and 0.9107 respectively. The registration performance of GAN-Q-Unet is compared with the state-of-the-art techniques and it shows the efficiency of the proposed 3D image registration.

1. Introduction

Scoliosis is described as a 3D deformity of the spine which is considered by both vertebral rotation and lateral curvature. Severe cases of scoliosis affect lungs and heart which leads to breathing problem and making the function of heart complicated. It improves the possibility of lung infection as well as heart failure. The geometry of 3D spinal is required by the scoliotic clinics, for the evaluation, prediction and treatment of scoliosis [1,2]. Commonly used pre-operative 3D images including Magnetic Resonance Imaging (MRI), Computer Aided Design (CAD), CT, and Cone-beam CT (CBCT). The spine procedures with intra operative images involve high radiation and it is expensive. The complex structure of spine consist of vertebra, intervertebral discs, ligaments, 6 Degrees of Freedom (DOF), muscles and zygapophysial joints which leads to the pose measurement of spine challenged. Such information's are used to quantify the scoliotic deformities in spine curvature [3]. Frequent and accurate registration of 3D image is required for the prediction of scoliosis [4]. 2 d to 3 d registration is widely used in clinical procedures such as Minimally Invasive Surgery, Image Guided Endoscopy, Image Guided Radiotherapy, and Interventional Radiology.

In the same coordinate system, the intra operative 2D and pre-operative 3D can be considered for accurate disease diagnosis [5]. Spine registration is a process of transforming several groups of data into the single coordinate system. The integrated image resolves the issue related to scale, skew and rotation. The accuracy of spine registration is reduced with the variation of large spine posture between surgical intervention and image acquisition [6]. In order to detect the geometric variations of intervertebral discs, the motion patterns of joined intervertebral location is accurately estimated. It tackles the relevant clinical issues for evaluating the adjacent vertebrae pattern of surgical fusion. Based on the geometric centroid, the body anatomy of each vertebra is measured. The connecting parts of intervertebral head movement is based on vertebra geometry, soft tissues constraints and the spine curvature [7,8]. For constructing spine profile from undeformed

* Corresponding author.
E-mail addresses: gadusrinivasarao5@gmail.com (S.R. Gadu), cpothala@gitam.edu (C. potala).

https://doi.org/10.1016/j.health.2023.100251
Received 25 April 2023; Received in revised form 3 July 2023; Accepted 30 August 2023
Available online 31 August 2023
2772-4425/© 2023 The Authors. Published by Elsevier Inc. This is an open access article under the CC BY-NC-ND license (http://creativecommons.org/licenses/by-nc-nd/4.0/).

configuration, mid-sagittal plane of the spine is estimated. For each lumber disc, the cross sectional area is digitally estimated with mid height plane [9].

Single view registration uses the point to plane perception with depth aware 2D to 3D registration. To enhance the depth perception or to get additional 3D information, the x-ray images are incorporated with 3D images [10]. While considering the regions, they are challenged due to nerve proximity, narrow joint space and deep location. It affects the process of accurate projection with the current standard of CT or fluoroscopy. This image modality causes several limitations because of ionizing radiation to the patient [11]. To enhance the clinical usage of registration approaches, it is essential to consider the issues of registration capture range and registration accuracy. The accuracy of registration is based on aligning error between preoperative volume and intraoperative anatomy even permitting the successful registration of automatic approaches [12]. Several registration approaches are based on the spatial connection and image dimension for 3D registered images [13]. After registration, the 3D error is measured in 3D Slicer interface for facilitating translation in clinical studies [14]. The 3D registration algorithms are limited due to its interactivity, complexity and sensitivity [15].

The approaches based on intensity and feature is commonly utilized for the registration of spine image. Fiducial markers and anatomical structures of the spine is used in feature based approach in which surface extraction and feature points are segmented [16]. To detect the causes of spinal axial parameters of clinical spine measurements, the measurement between 2D and 3D radiology is evaluated with the sagittal and coronal parameters of spine. These parameters are depends on the spinal parameters of the transverse plane [17]. From the collection of prior models, the characteristic factors and deformable mean models are extracted with statistical model based approaches. Based on mean model status, the statistical model based techniques are categorised as statistical shape model (SSM) and statistical intensity model (SIM). SSM uses shape model whereas the SIM uses the intensity for mean model. There are three major components in Active Appearance Model (AAM) namely template intensity image, statistical shape model and template bone surface [18].

The machine learning based algorithms are utilized for automatically detecting scoliosis based on segmentation [19,20,21]. In classical methods, capture range and the robustness is provided with the need of better initial alignment and uniform data. In this technique, artificial neural network (ANN), models an artificial agent which is trained for learning policy with the optimal strategies based on input images. Because of high robustness, the interventional guidance are applied in which more robustness is provided than valuable accuracy. The optimization based approaches are widely used with the simulated x-ray which is obtained from 3D x-ray attenuation map [22]. Artificial Intelligence (AI) based cross modality registration is used recently with the challenges of requiring large training data for ground truth (GT) registration. It can be worked only on the specific modalities where they are trained [23,24].

The deep learning based approaches are recently used with digital radiography (DRR) of the spine image. The mutual registration approach based on adaptive grid is developed [25] with the optimization of control points. The complex spinal deformities are measured based on Cobb angle. It is enabled with the analysis of quantitative surface deviation for accessing the 3D spinal model [26]. The progression of curve is measured from the extracted x-ray image. The volumetric model of human spine is generated and it is divided into various tissues for vertibra and intervertibral disc [27].

The new inpainting model is developed with GAN model which focuses on structure and similarity coherence of the image with the learning capability of expression. Inpainting is a process of reconstructing the image with some additional information. The image is restored by filling the missing parts of image in inpainting process. For enhancing the quality of inpainting technique, it requires to deal with the information related to missing content. The new inpainting algorithm is proposed for 2D to 3D registration of image in a more accurate way. The contribution of the proposed work is described as follows.

- ➢ In order to predict the complex structures from large images, the new inpainting algorithm is proposed with the concept of hybrid quantum neural network. The novel inpainting algorithm based on GAN network model is developed based on U-net and Quantum Neural Network (QNN) for obtaining better registration of 2D to 3D image.
- ➢ The input image is preprocessed to create synthetic data which enhances the bone regions and it improves the accuracy of registration framework. The proposed inpainting algorithm improves the capture range of 2D-3D registration for X-ray and spinal CT images.
- ➢ The discriminator is replaced with U-net in which better data representation is provided rather considering incoherent structural or geometric patterns. The proposed algorithm is used with realistic images having some variants, shorter inference time, and it handles irregular hole patterns.
- ➢ The discriminator network is modelled with QNN based U-net block structure which is used for learning the network.

The organization of the paper is given as follows. Section 2 provides the related work, proposed methodology is presented in section 3, the experimental evaluation is given in section 4 and conclusion is given in section 5.

2. Related work

The work related to the proposed 2D to 3D registration process of spine x-ray image is described as follows.

B. Aubert et al. [28] had proposed convolutional neural network (CNN) approach for fitting realistic statistical shape model of the spine into x-ray images. An adolescent idiopathic scoliosis dataset with 400 patients and the mean Cobb angle of 43° was collected from the Saint-Justine University. CNN automatically adjust and detects anatomical landmarks by controlling spine deformation model with gradual and hierarchical iterative process.

Shun Miao et al. [29] had discussed agent based approaches for the registration of medical images and were implemented with Spine and Cardiac dataset. Learning based image registration was developed by employing DNN to analyse images for estimating plausible registration. The registration accuracy of 92% was obtained for spine image and 100 was obtained with cardiac image.

Nima Masoumi et al. [30] had proposed two patch-based rigid image registration technique and was evaluated with CT images provided by The Cancer Genome Atlas Sarcoma (TCGA-SARC). It depends on the correlation ratio (CR) and normalized cross-correlation (NCC) for registering misaligned Ultrasound (US) and CT images.

Andrew chan et al. [31] had proposed CT-3 Distinctness, Uniformity and Stability (DUS) registration method based on pre-alignment phase including vertebral symmetry information for registering preoperative CT model. The experimental setup involved a custom 3DUS system that was developed by combining four Optitrack Prime 13 W motion capture cameras (NaturalPoint, Corvalis, OR, United States) and an Ultrasonix SonixTablet (BK Ultrasound, Peabody, MA, United States) with a L14-5/38 linear transducer. The 3DUS initially reconstruct the vertebral surface and it was registered with preoperative registered model which leads to surface localization with 98.2% accuracy.

Roman Schaffert et al. [32] had investigated weighting scheme with learning for enhancing the performance of registration. The Spine dataset was utilized in which attention based model was learned to get higher attention by suppressing the corresponding outliers. Success rate of spine registration was improved with 97% with learning based approach and attained re-production distance of 0.5 mm mean.

Jun Soo Lee et al. [33] had developed GAN inversion approach for feature extraction and the feature vectors were classified with Multi

Table 1
Comparison of conventional approaches.

Techniques	Research gaps	Training percent	Testing percent	Parameters
CNN	Obtaining geometrical information to fit the 3D model's projection in radiographs.	81%	19%	Mean Average Error (MAE) = 1, Root Mean Square (RMS) = 1.4.
Agent based techniques	Analysing the images with deep learning paradigm for image registration.	Spine = 94%, Cardiac = 97%	Spine = 6%, Cardiac = 3%	Glomerular Filtration Rate (GFR) = 2.1, Median = 1.19, Runtime = 2.6s
Two patch-based rigid image registration method	More realistic view of the vertebrae is provided with preoperative planning and simulation.			fiducial registration errors (FRE) = 1.31 and 0.93for Canine and Lamb phantom.
CT-to-3DUS	Developing feasible image registration algorithms with pre-operative 3D-CT images of individual vertebrae.			Registration error = 0.66 to 2.3.
Attention based deep learning	Performing data training with different angles and providing refinement for higher accuracy.	80%	20%	CR = 11 mm, Success rate (SR) = 77.3,

Layer Perceptron (MLP) for detecting scoliosis. The representation of scoliosis was learned with semi supervised GAN by Lee W et al. [34]. Zhongyi Han et al. [35] had performed automated segmentation and classification with Spine-GAN. Better generalization and reliable performance was achieved with error prediction capability.

Ching-Juei Yang et al. [36] had proposed X2CT-GAN for developing 3D-GAN of the spine. From simulated x-ray images, the spine structure was extracted with varying bone signal conditions. For detecting scoliosis, the spine curve is segmented with the rotation of vertebral. For segmenting bony features, Weiwei Jiang et al. [37] had suggested ultrasound global guidance block network (UGBNet) based scoliosis visualization. By combining the significant of x-ray and ultrasound imaging modalities, Weiwei Jiang et al. [38] had proposed an ultrasound to X-ray synthesis generative attentional network (UXGAN) for synthesizing ultrasound images.

For efficiently utilizing data samples, the data augmentation based training strategy is proposed by Olaf Ronneberger et al. [39]. Jonathan Long et al. [40] had invoked efficient interference and learning with fully CNN. The classification networks were included with fine tuning of segmentation tasks by transferring the learned representation.

The comparison of existing approaches is given in Table 1.

In recent researches, the 3D registration is accomplished based on the approaches such as CNN, agent based techniques, two patch based rigid registration, CT to 3DUS and attention based approaches. These algorithms are developed based on the 3D measurements of clinical sharing, providing robustness, and for improving accuracy. But the registration accuracy is affected with registration error, lack of 3D information and testing deformation etc. The proposed inpainting algorithm tackle this issue by developing a novel network model based on GAN. The matching of 3D volume to 2D image is challenging due to long computation times, discrepancies in imaging modalities, and patient movement. Due to lack of 3D information, establishing required

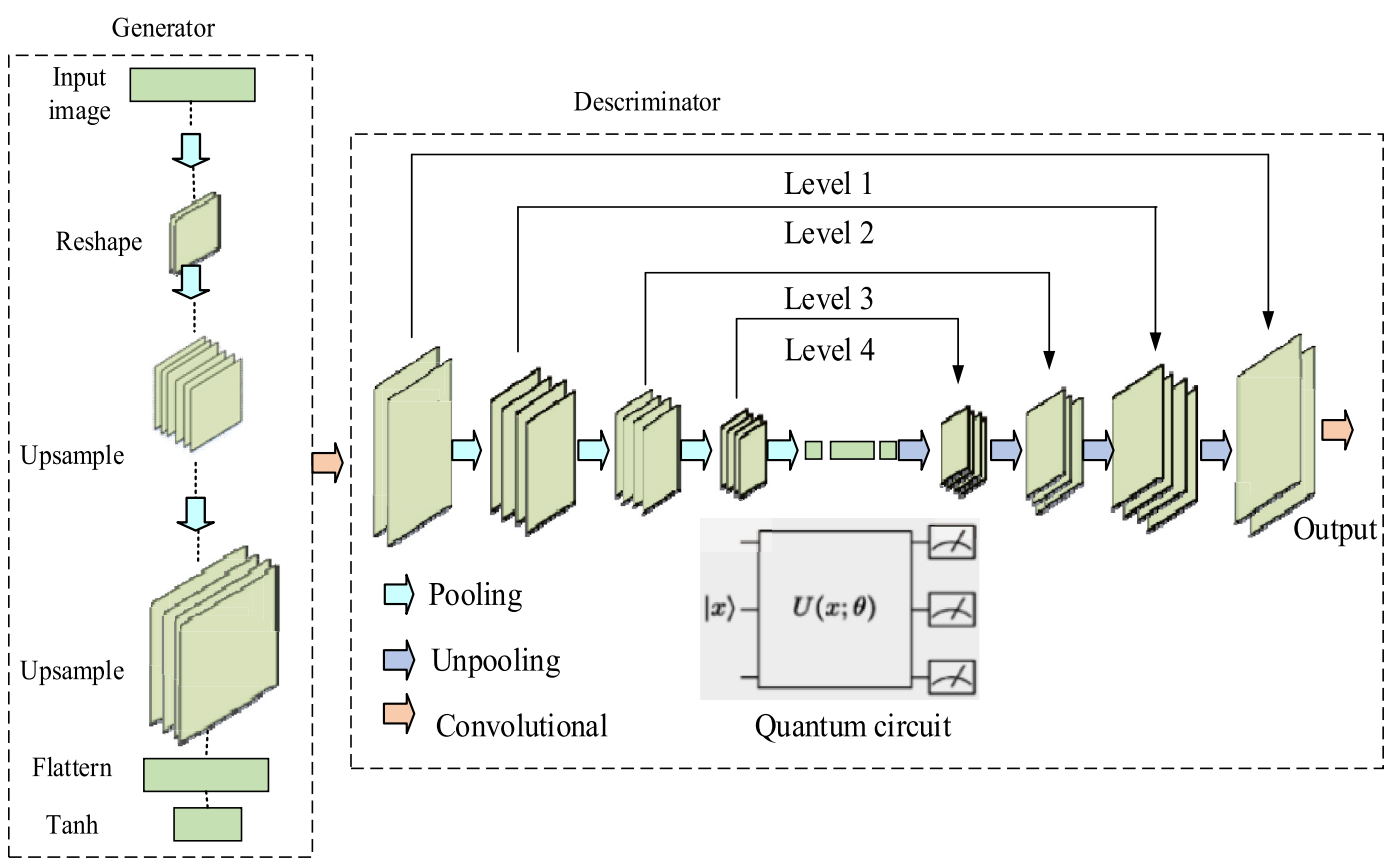

Fig. 1. Architecture of proposed GAN-Q-Unet system for 2D to 3D registration.

geometrical information for 3D reconstruction is considered as a major issue. In order to fit the 3D registration model with 2D information, the inpainting algorithm of 3D increases the complexity. It is challenged to determine the relationship between the intra operative structure and preoperative structure of the image in 2D to 3D registration. The accuracy can be improved using the deep learning model with better data representation and enabling exponential speedup for the algorithm. The parameters such as.

3. Proposed method

The proposed GAN model consists of generator and discriminator network. The generator network converts the random input into data instance. This data instances are classified with the discriminator. Due to the variation in learning of global and local images, the discriminator will not provide better representation for data. It causes mottled or discontinued local structure in the generated image. It can be resolved and to get output simultaneously from local and global pattern of the image, the discriminator architecture is modified with U-net. U-net is an encoder decoder CNN in which the encoder is responsible for down sampling and decoder is responsible for upsampling. The encoder minimizes the spatial dimension in each layer. In between encoder and decoder network, skip connection is used. The progressive upsampling matches the output resolution with input to ensure precise localization. In between the matching resolution of two modules, the data is routed through skip connection which improves the accuracy of the network. The new structure of U-net is modelled with QNN. It has the generalization capability of learning unknown unitary quantum transformation. The learning capacity also improved with the proposed registration model. Overall architecture of the proposed system is shown in Fig. 1.

From the given x-ray image, synthetic image is computed with the x-ray propagation which causes decrease in energy. The attenuation in energy is based on the attenuation coefficient and distance travelled. This relationship can be modelled as Beer Lamberts Law and the intensity I_n is represented as,

$$I_n = I_b \exp^{Acx_1} \tag{1}$$

Where, I_b represents the incident beam, Ac represents the attenuation coefficient and x_1 is the travelling distance. For each volume of CT voxel, the attenuation coefficient is computed for the simulation of x-ray generation process. Each voxel is denoted with the value of Hounsfield unit (HU) which is obtained by applying linear transformation to the attenuation coefficient. Hence, the information related to linear attenuation is preserved. The parallel projection model is considered for estimating average attenuation coefficient with the y-axis range of $[1 - M]$. Where M represents the pixel length of x-ray image. By representing the image (x_1, y_1, z_1), the average attenuation map for 3D image is estimated as,

$$\eta_{avg}(x_1, y_1, z_1) = \sum_{y_1=1}^{M} \frac{\eta_{wa}\left(H(x_1, y_1, z_1) + 10^3\right)}{\left(M.10^3\right)} \tag{2}$$

The simulated x-ray is computed with the generation of Beer Lambert's law as follows.

$$\mathrm{Im}_{syn}(x_1, z_1) = \exp^{\gamma.\eta_{avg}(x_1, y_1, z_1)} \tag{3}$$

Where, η_{wa} represents the attenuation coefficient. The Simulated X-ray computed in which it matches the original input x-ray images. The bone region of the image is detected based on image intensity. Therefore the intensity of the image is represented and enhanced with the use of Beer Lamberts Law. The input image is converted into simulated x-ray using Beer lamberts Law by enhancing the bone regions. The enhanced image is fed into the proposed GAN-Q-Unet model for image registration.

3.1. U-net

Unet is highly utilized to resolve the issue of image transformation problem in the research of image registration. For each decoder level, the output is computed as follows.

$$Y^j = G\left(y^J - 1\right) \oplus Z^j \tag{4}$$

In the jth encoder level, the skipped connection is represented as Z and the concatenation operation is denoted as $\oplus$. Removing the skipped connection reduces the accuracy it show that the model is based on the skipped connection of the network. Upsampling is responsible for enhancing the image size. After upsampling the upper level produces the image with same size. In the discriminator encoder module is represented with E_D and decoder module is denoted as D_D. Based on the decision from encoder and decoder, new loss for the discriminator is estimated.

$$L_E = L_{E_D} + L_{D_D} \tag{5}$$

From the output of encoder, the encoder loss is computed as,

$$L_{E_D} = -F_y[\log E_D(y)] - F_a[\log(1 - D_D(H(a)))] \tag{6}$$

By using the mean decision of overall pixel, the loss for the decoder is computed as,

$$L_{D_D} = -F_y\left[\sum_{j,k} \log\left[E_D(y)\right]_{j,k}\right] - F\left[\sum_{j,k} \log\left(1 - \left[D_D(H(a))\right]_{j,k}\right)\right] \tag{7}$$

Where, $[E_D(y)]_{j,k}$ and $[D_D(H(a))]_{j,k}$ refers the discriminator decision at pixel (j, k). This pixel level outputs are obtained from the higher level feature's global information. From the process of upsampling more local information is obtained from low level features. Both features are mediated with the skip connection between intermediate layers.

In Unet based architecture, increasing the number of layers slow down the learning process.

Each layer adds some specific feature for the learning process. This feature learning makes the entire process to slowdown. Hence it requires eliminating several layers for abstract feature representation. To avoid this, the layers of U-net are replaced with quantum layers. The quantum circuits are simulated in NN with quantum states via Deep Boltzmann Machine (DBM). For retrieving the information, quantum layers use qubits or quantum bits. Unlike other classical algorithms, this can store multiple values at the same time to make learning faster.

The boltzman machine has hidden and visible binary units which are represented with $a_b, b = 1, \ldots, P$. Where, the total units are represented with P. To maintain consistency with quantum mechanics, the probability distribution $a_b \in \{-1, +1\}$ is used rather using $a_b \in \{0, 1\}$. For the linear distribution of the parameters, the probability distribution is identical. The hidden and visible states are differentiated with the normalization $a_b = (a_w, a_j)$, where w and j represents the index of and visible and hidden states. The visible, hidden and the combined units are represented with $w, i,$ and $a = (w, i)$.

The classical energy equation is replaced with the equation of quantum bits. The principle of quantum mechanics depends on matrices and the dimensionality is same as that of the amount of possible states (2^P). The number of variables used in common machine learning approach is equal to the dimension of the quantum vectors. The energy function is replaced with Hamiltonian matrix with $2^P \times 2^P$ diagonal matrix [41].

3.1.1.

The GAN network consists of two components namely generator and discriminator. For learning the distribution P_a with input data y, it is assumed that the true samples are enables with data distribution P_a and noise $Q_a(a)$. The random noise is accepted as input and it generates

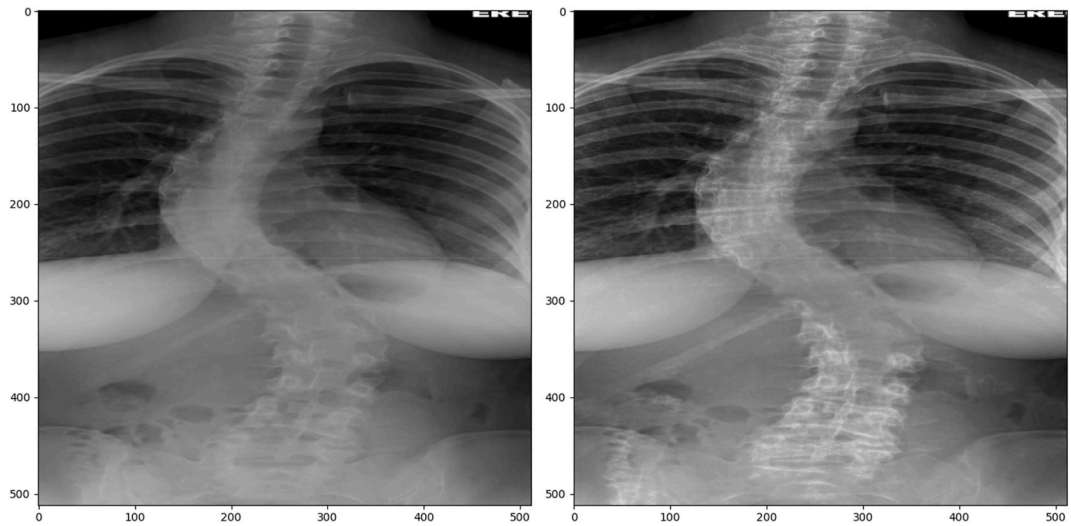

Fig. 2. The input x-ray image (left side) and the 3D registered output image (right side).

Table 2
Comparison of proposed and existing approaches with GCOR, JHMI, MAMI, MESQ, SSIM, and DSC.

Techniques	GCOR	JHMI	MAMI	MESQ	SSIM	DSC	PSNR	Loss
Proposed	0.0051	0.0021	0.1165	0.0844	0.9395	3.0564	28.90	0.8939
GAN-Unet	0.0041	0.0047	0.085	0.104	0.925	2.24	27.98	1.02
CNN [43]	0.003	0.006	0.061	0.112	0.005	0.943	26.51	1.36
GAN [44]	0.0067	0.0087	0.035	0.152	0.9135	0.8068	25.30	1.20
PatchMatch [45]	0.003	0.0095	0.035	0.123	0.865	0.695	27.51	1.16
Contextual Attention (CA) [45]	0.0056	0.0097	0.065	0.125	0.893	0.985	24.36	2.41
Globally and Locally Consistent Image Completion (GLCIC) [45]	0.003	0.0098	0.065	0.136	0.862	0.965	23.83	2.66
EdgeConnect [45]	0.005	0.045	0.085	0.125	0.920	0.958	27.95	1.50
statistical deformation model (SDM) [46]	0.002	0.032	0.068	0.321	0.327	0.921	25.31	1.51

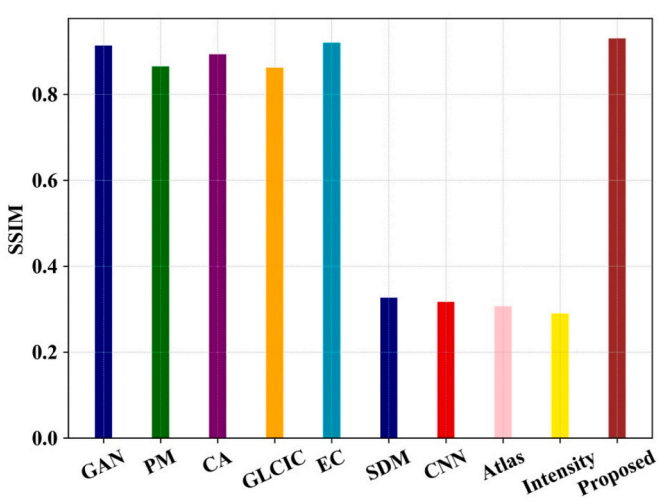

Fig. 3. Comparison of SSIM performance with existing approaches.

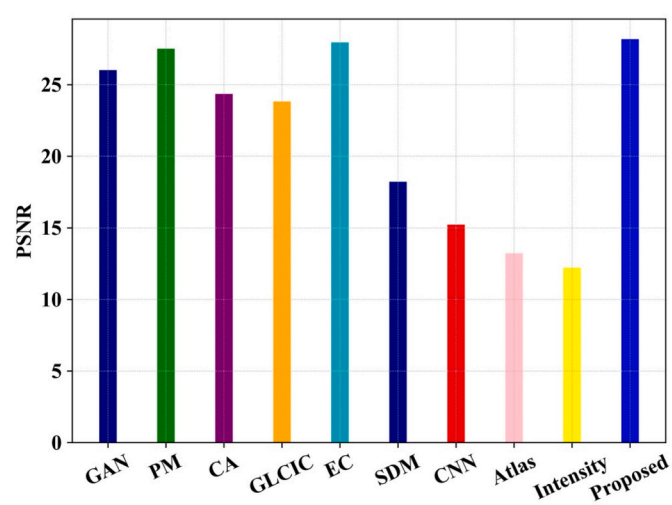

Fig. 4. Compariosn of PSNR performance with existing approaches.

mapping to database $H(a)$. The $E(y)$ computed the probability y which is a true sample of training data. While using optimization procedure, the discriminator is trained to enhance $\log E(y)$ in which the probability of correct label is assigned with the proper source when the generator minimizes $\log(1 - E(H(a)))$. Hence the objective is based on resolving minimax problem. The generator is based on the objective of generating image to fool the discriminator with the input distribution of P_a. The training of GAN is represented as follows.

$$\text{minmax } W(E,H) = F_{y\sim Q_{data}(y)}[\log E(y)] + F_{a\sim Q_a(a)}[\log(1 - E(H(a)))] \quad (8)$$

Where, H represents the generator, E represents the discriminator, $Q_a(a)$ is the input noise, y represents the image data, $Q_{data}(y)$ denotes the representation of original data. The adversarial modelling framework of min and max is used with multiple components. The output of generator and discriminator network is described as $E(.)$ and $H(.)$ and the Gaussian noise vector is used as an input for the generator.

The generator is trained and considering the synthetic images are real,

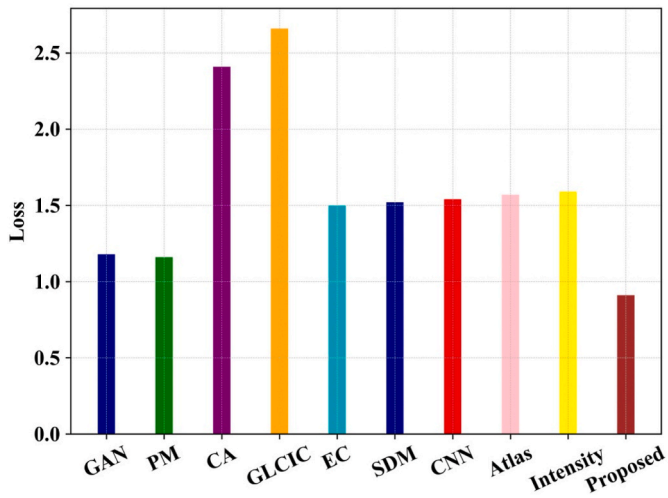

Fig. 5. Comparison of registration loss with existing approaches.

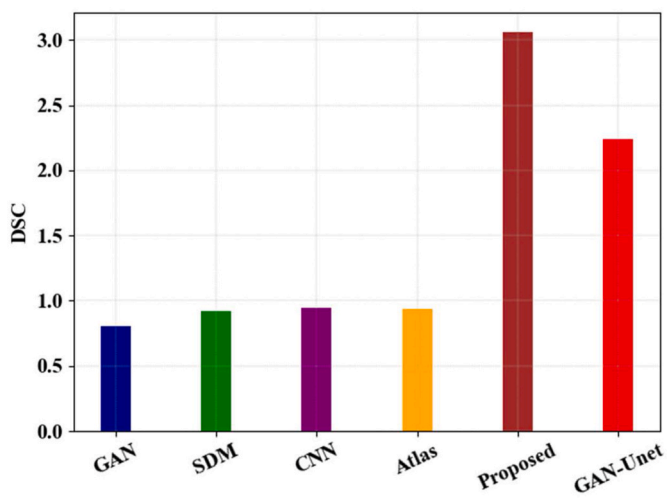

Fig. 6. Comparison of GAN-Q-Unet registration performance with DSC metric.

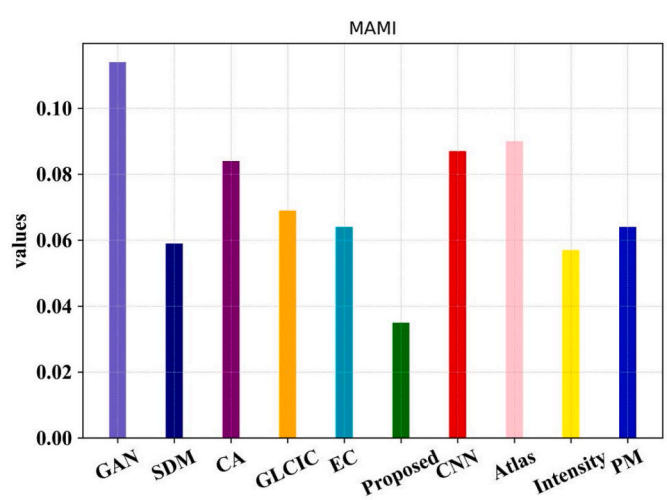

Fig. 7. Comparison of GAN-Q-Unet registration performance with MAMI.

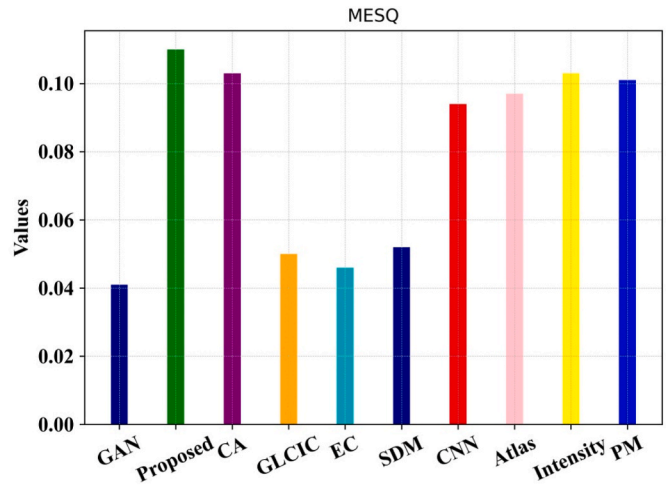

Fig. 8. Comparison of GAN-Q-Unet registration performance of MESQ.

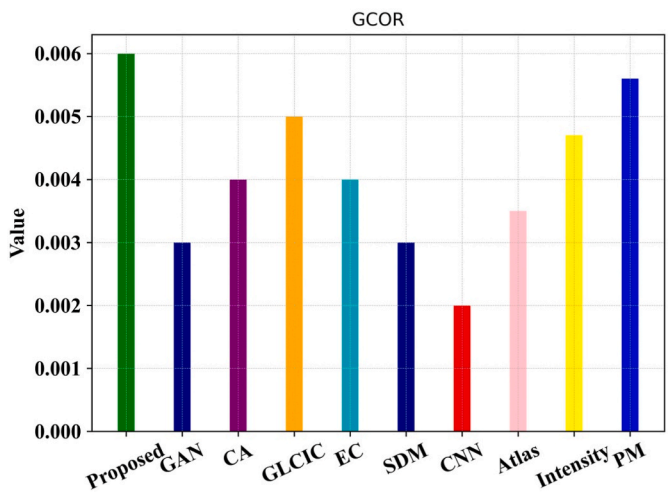

Fig. 9. Comparison of GAN-Q-Unet registration performance with GCOR.

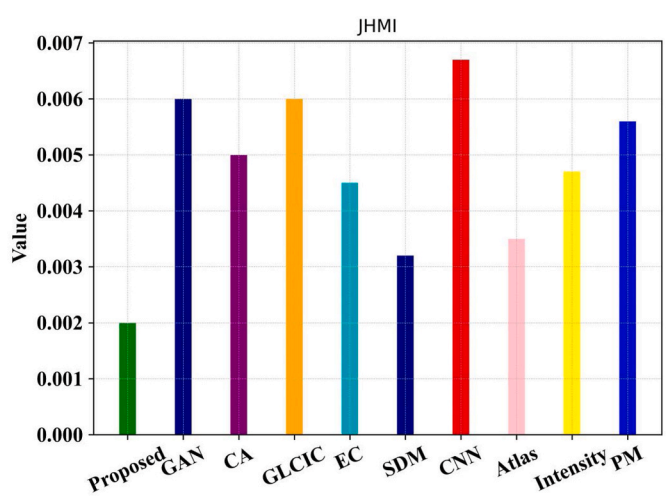

Fig. 10. Comparison of GAN-Q-Unet registration performance with JHMI.

Table 3
Comparison of proposed approach with other deep learning approaches.

Techniques	GCOR	JHMI	MAMI	MESQ	SSIM	DSC	PSNR	Loss
Proposed	0.0051	0.0021	0.1165	0.0844	0.9395	3.0564	28.90	0.8939
GAN-Unet	0.0041	0.0047	0.085	0.104	0.925	2.24	27.98	1.02
GAN	0.0040	0.0050	0.059	0.256	0.9135	0.8068	27.35	1.20
Auto encoder	0.0037	0.0054	0.075	0.241	0.865	1.256	27.51	1.16
Bi-LSTM	0.0039	0.0060	0.076	0.145	0.893	1.635	24.36	2.41
ResNet	0.0038	0.0051	0.075	0.198	0.862	1.987	23.83	2.66

$$L_H = -F_{a\sim P(0,1)}[\log(E(H(a)))] \tag{9}$$

The adversarial loss of the overall network is described as,

$$L_{ad} = L_E + L_H \tag{10}$$

3.1.1.1. Advantages and disadvantages of GAN. GAN generates new version of image which is similar to the original image. The generated data is not easily distinguishable from real data. GAN can be processed with the details of data and the interpretation is easily carried out for machine learning work. The recognition of data points is easy with GAN based network due to the possibility of computing distance between data points. GAN can enhance the data quality by minimizing the noise and clearing the error associated.

Different kind of data is required to check the accuracy of the work and it makes the training process harder. It can be resolved with the skip connection of Unet architecture and the QNN layers. The use of QNN improves the training process by storing multiple values at the same time. Generating results from test or speech is complicated. In this paper, the spine image is processed and it is not applicable.

3.1.2. DSC

It estimates the similarity from two set of data. It can be measured by dividing the overlapping area between the images with total number of pixels in both images.

$$D_{SC} = \frac{2|x_1 \cap x_2|}{|x_1| + |x_2|} \tag{11}$$

Where, x_1 and x_2 are input and predicted images.

3.1.3. QNN

In quantum computing each unit is represented as qubits. The notation ket $|.\rangle$ is used to represent object in column vector. The complex conjugate transpose is denoted as $\langle .|$. In two dimensional Hilbert space H_s^2 two level quantum system is represented as $\{|0\rangle, |1\rangle\}$ which is a single qubit and it can be represented as,

$$|\varphi\rangle = \beta|0\rangle + \gamma|1\rangle \tag{12}$$

In equation (11), β and γ represents the complex numbers.

$$|\beta|^2 + |\gamma|^2 = 1, \beta, \gamma \in H \tag{13}$$

The universal quantum gates are selected with single qubit rotation axis, controlled rotation axis and Hadamard gate.

The Hadamard gate operation is modelled as follows.

$$Ha\Big|0\rangle = \frac{1}{\sqrt{2}}(|0\rangle + |1\rangle), Ha|0\rangle = \frac{1}{\sqrt{2}}(|0\rangle - |1\rangle) \tag{14}$$

Where, Ha represents the qubits of the system. In between two states, the density matrix α_{BC} is denoted as,

$$\alpha_B = Pt_C(\alpha_{BC}) \tag{15}$$

Where, Pt represents the partial trace over C, and the partial trace is represented as,

$$Pt_C(|b_1\rangle\langle b_2| \otimes |c_1\rangle\langle c_2|) = |b_1\rangle\langle b_2|Pt(|c_1\rangle\langle c_2|) \tag{16}$$

Where, b_1 and b_2 represents the vectors of B, c_1, c_2 are vectors of C, and C, B represents the finite dimensional vector space. By adding QNN with U-net, the cost function is improved. In each layer, the perceptron nodes are represented with qubits. The number of nodes at each layer is denoted as p_m and it is considered that, $p_{m-1} < p_m$ for $m = 1, 2, \ldots M$. The input layer is represented with $M = 0$ and $m = M + 1$ relevant to the output layer. The input and output state is denoted with $\alpha^{m_{in}}$ and $\alpha^{m_{out}}$. The layer $m + 1$ of output state denotes the addition of output with the input state layer m. Addition operation denotes the matrix element wise addition operation. Since $p_{m-1} \leq p_m$, the tensor product is applied to $\alpha^{m_{in}}$ and $|0\ldots0\rangle\Delta_{n_m}\langle 0\ldots0|$ for keeping same direction. The U-net is constructed with M quantum perceptron layers. The quantum layers are constructed based on DBM and the transitions between layers are accomplished through multiple layer perceptron. For the input qubits, the input state is represented as $\alpha^{m_{in}}$ and the output qubit of mixed state $\alpha^{M+1_{out}}$ is obtained with unitary operator V^m which is in the form of quantum perceptron's matrix product. It is defined as,

$$V^m = V^m_{nm} V^m_{nm-1} \ldots V^m_1 \tag{17}$$

In layer m and $m - 1$, V^m_k described as qubits. The unitary operators are arbitrary and are not varied. Hence, the order is essential in the unitary layer. When the information is processed from $\alpha^{m_{in}}$ to $\alpha^{M+1_{out}}$, the new input state is generated with $m + 1$ layer by adding the input state with output state layer m for all $m = 1, 2, \ldots, M$. In between the unitary and hidden layer, the layer unitary is provided with $V^1 = V$. The x-ray image is improved in which the bone region is estimated to enhance the quality of image. By using proposed methodology, low-cost, high-quality, faster, and accurate 3D spine reconstruction can be achieved.

4. Experimental evaluation

It is not possible to gather original x-ray and corresponding CT images for 3D registrations. For simulating x-ray images, tomographic iterative Graphics Processing Unit (GPU)-based Reconstruction (TIGRE) is utilized. The TIGRE is utilized for simulated x-ray generation from various projection view. Hence, the 3D information is required for the registration process. The blurred appearance of x-ray image is improved and simulated x-ray is obtained with enhanced bone regions.

4.1. Dataset description

The dataset contains 609 anterior-posterior spinal x-ray images and it was created by the professionals of London Health Sciences Center (http://spineweb.digitalimaginggroup.ca) [42]. Based on four corners, each vertebra is placed with four landmarks. These landmarks will be utilized for the computation of Cobb angle. Based on our data access request, the dataset is provided by spineweb platform. These images can also used for the task of scoliosis detection by measuring cob angle.

4.2. Performance evaluation metrics

The performance of the proposed work is evaluated with the metrics described as follows. These performance metrics are used in the previous work for estimating the registration performance. The new metrics were

added in the work for showing the better registration framework in different point of view.

a PSNR

PSNR focuses on the maximum data contribution to data when compared with noise which affects the representation of image. It can be estimated as,

$$P_{SNR} = 10\log_{10}\left(P^2\right) / E_m \tag{18}$$

Where, P represent the peak value of the image and E_m is the mean square error computed from the image.

b SSIM

It quantifies the degradation of image quality due to data transmission caused by 3D registration. It requires that two images are taken from same shot and both should be identical. The structural similarity of second image is computed from the first image which has different quality. SSIM is computed as,

$$E_s(x_1, x_2) = \frac{(2\lambda_{x_1}\lambda_{x_2} + d_1)(2\eta_{x_1x_2} + d_2)}{\left(\lambda_{x_1}^2 + \lambda_{x_2}^2 + d_1\right)\left(\eta_{x_1}^2 + \eta_{x_2}^2 + d_2\right)} \tag{19}$$

Where, λ represents the mean, η is the standard deviation, d_1 and d_2 represents the constant values.

c Gradient Correlation (GCOR)

It is calculated based on the horizontal and vertical image gradient. The GCOR for the image is described as follows.

$$E_G = \frac{\sum_j (a_1(j) - b_{a_1})(a_2(j) - b_{a_2})}{\sqrt{\sum_j (a_1(j) - b_{a_1})^2} \times \sqrt{\sum_j (a_2(j) - b_{a_2})^2}} + \frac{\sum_j (c_1(j) - b_{a_1})(c_2(j) - b_{a_2})}{\sqrt{\sum_j (c_1(j) - b_{a_1})^2} \times \sqrt{\sum_j (c_2(j) - b_{a_2})}} \tag{20}$$

Where, b represents the mean pixel value a_1 is the horizontal image gradient of input image, a_2 is the horizontal image gradient of 3D registered image, (c_1, c_2) represents the vertical image gradient of input x-ray image and 3D registered image.

d Joint Histogram Mutual Information (JHMI)

JHMI describes the capacity of one image describing another image and the higher metric represents the high similarity and lower the metric value denotes the lower similarity. JHMI can be described as,

$$E_J = S(x_1) + S(x_2) - J_S(x_1, x_2) \tag{21}$$

Where, S represents the Shannon–Weiner entropy of the image, x_1 is the original image, x_2 is the output image, and J_s represents the joint Shannon–Weiner entropy.

e Mattes Mutual Information (MAMI)

MAMI utilizes unique set of pixel location instead of selecting new set in each iteration. From two images the joint probability distribution of sampling images are utilized to estimate certainty of set of pixels map to the same value in other image. High reductions of entropy between two images are denoted with high mutual information. MAMI implementation is similar to JHMI but the probability distribution is computed based on Parzen histograms instead of Shannon–Weiner entropy.

f Mean squared error (MESQ)

It represents the average pixel variation among the entire image. The higher MESQ indicates that the variation is high and lower MESQ represents low variation between images.

$$E_m(x_1, x_2) = \frac{1}{M}\sum_{i=1}^{M}\left(|x_1 - x_2|^2\right) \tag{22}$$

Where, E_m represents the mean squared error, M represents the number of images, x_1 is the x-ray image and x_2 denotes the 3D registered image.

g Loss

Loss is described as the deviation in least absolute value. It reduces the sum of variations between original and predicted image. It is calculated as,

$$L = \sum_{j=1}^{m}\left(x_j - f(x_2)\right)^2 \tag{23}$$

Where, x_j is the input image and $f(x_2)$ represents the values of predicted image.

4.3. Results and discussion

The proposed GAN-Q-Unet for 2D to 3D registration was implemented with the working platform of Python with the software configuration of Windows 10 pro. The hardware configurations used are Intel (R) Core(TM)2 Duo CPU E8400 @ 3.00 GHz 2.99 GHz processor, 195 GB storage, 8 GB RAM, and SVGA monitor with resolution 1024 × 768. Among 609 Spineweb x-ray images, 80% is used for training and 20% is used for testing. The proposed 3D registration is implementedwith spine web dataset.

Initially, the libraries such as numpy, tensorflow. keras, and matplotlib are imported for transforming, preprocessing and generating the neural network model. Then the dataset is loaded and it is already divided into training and testing set. The images are readed, processed, predicted, and the results are plotted with imread (), load_image (), load_model (), and imshow () functions. Then the generator model is created with the latent dimension 100, dense laye, batch normalization layer, tanh activation function, momentum 0,7, and alpha 0.2. Adam optimization algorithm is used in the GAN model. Then the discriminator model is created based on Unet. In Unet encoder blocks, decoder blocks and skip connection are created with encoder_block (), decoder_block (), and concatenate () functions. For QNN implementation, the tensor flow quantum is installed and then the resource package is modified to latest version. The module dependencies such as sympy, and cirq is added. From tf. keras.Layer, the circuit layer is inherited and the circuit layer is defined with 'Circuit'. The functions such as GridQubit (), AddCircuit () is added for using the quantum layer. Finally, the generated model is compiled to produce the output.

The attenuation coefficient is considered 0.2 CM^{-1} and the γ value is chosen as 0.02. The architectural parameter used in the proposed work is based on the performance of previous researches. With this parameters, the algorithms has provided better results in the existing researches. The proposed work is compared with the existing approaches from Hooman Esfandiari et al. [43],Ching-Juei Yan et al. [44], Qi Sun et al. [45], Jeroen Van Houtte et al. [46]. The generator and discriminator architecture has been developed with the resolution of 256 × 256 and 128 × 128 with the channel multiplier 64. The input images are down sampled with the feature map dimension of 4 × 4. The initial learning rate is set to 0.002, the activation function tanh is used with the droupout parameter 0.5. The input image and the registered image with GAN-Q-Unet is given in Fig. 2. The comparison of result of proposed and existing approaches is given in Table 2.

The SSIM comparison for the proposed work is shown in Fig. 3.

Structural similarity is compared with the existing approaches such as GAN, Patchmatch, CA, GLCIC, EdgeConnect and SDM. When compared with all approaches low SSIM is obtained for SDM technique whereas the higher SSIM is obtained with our proposed approach. For the other approaches, the SSIM is obtained above 0.8 and it is reached up to 0.9. Except SDM, other existing approches provide slight variation in performance. When incresing th SSIM, better registraton capability is obtained. Similar to that, reducing SSIM reduces the registration performance.

The PSNR comparison for the proposed work is shown in Fig. 4. The proposed PSNR is compared with the existing approaches such as CA, EdgeConnect, PatchMatch and GLCIC. The overall performance for all 3D registration approaches lies between 23 and 29. But in case of proposed approach, the higher PSNR performacne is obtained and it is nearer to 0.99. The lower level of PSNR is attainedwith CA and GLCIC which is lower than 25 dB. The approaches like PatchMatch, EdgeConnect and proposed reaches the value of higher PSNR. The higher PSNR represents better performance of 3D registration whereas the lower PSNR represents the poor performance. The GAN-Unet provides lower performance than our proposed system.

The loss performance of the proposed GAN-Q-Unet3D registration is shown in Fig. 5. It determines the presence of error in the final registered image. The proposed approach has the loss performance lower than 1 and for the existing approches it is higher than 1. The proposed loss is compared with the registration loss of PatchMatch, CA, GLCIC, EdgeConnect and GAN-Unet approaches. The lowest registration perormance is obtained with GLCIC based technique whereas the higher performance has been obtained with proposed approach. For the approaches such as Patchmatch and EdgeConnect, the registration loss is lower and slight deviation from the proposed registration losss. The higher loss represents the higher error of 3D registration and lower loss represents the lower error of registration. The proposed performance is enhanced with the concept of quantum computing. Without using QNN, the performance is degraded than proposed approach.

The comparison of DSC performance for the proposed approach is shown in Fig. 6. For estimating the performance, the proposed work has been compared with the existing approches such as GAN, SDM, CNN, GAN-Unet and Atlas. Existing approaches are having the DSC result between 0.7 and 0.9 whereas the proposed approach has the DSC above 1. The proposed approach has been reached the higher result of DSC. The higher the result of DSC represents the higher registration performance and lower the DSC indicates the lower registration perormance.

The MAMI and MESQ performance comparison is given in Figs. 7 and 8. When comparing the MAMI of the proposed approach with CNN based and GAN-Unet approach, better performance is obtained with the proposed one. It reaches the range up to 0.10 whereas the CNN based approach has the MAMI result of 0.06. The MESQ performance of the proposed approach is compared with the existing CNN approach. When compared with the proposed approach MESQ is lower for CNN. The lower MESQ and higher MAMI indicates the best performance and the lower performance is represented with low MAMI and high MESQ.

The GCOR and JHMI performance comparison for the proposed and existing approaches are shown in Figs. 9 and 10. When compared with the existing approaches, higher performance has been attained with the proposed GAN-Q-Unet which has high GCOR and low JHMI. But for the existing approaches of CNN and GAN-Unet obtained slight lower performance in terms of GCOR and JHMI. The comparisons with other existing approaches are given in Table 3. The proposed approach is compared with GAN-Unet, GAN, Auto Encoder, Bi-Directional Long Short Term Memory Network (LSTM), and Residual Network (ResNet).

Our proposed 3D registration work outperforms all existing approaches in all metrics. It shows the ideal nature of the work and it is well suitable for scoliosis detection. The better results are obtained due to the GAN based framework which minimizes the error or loss by generating more artificial data similar to the real one. Also, the information loss is preserved with the skip connection of Unet layer.

4.4. Limitations

Even though the proposed approach has several advantages, it is limited with the data collection procedure. The real-time x-ray images are collected from the dataset. But it doesn't contain the 3D information. For the spine x-ray images, the corresponding CT images are not available for the registration framework. They image are manually created for synthetic data creation which enhances the bone regions of spine image. By analyzing the results, efficient performance is obtained with the proposed approach using manually generated image samples. Due to this data generation procedure, it has the possibility of missing essential details.

5. Conclusion

The exact information related to the 3D position of the patient without using radiation intensive intraoperative volumetric imaging can be enabled with image registration. The registration of 3D image is based on the given 2D X-ray image. The intra operative images will not provide additional 3D geometrical information. In this paper, the GAN model with U-net and QNN is proposed for the 3D registration of spine x-ray images. For enhancing the bone regions, synthetic data was created from the input image. Then the proposed GAN model is applied and the discriminator of the GAN was replaced with U-net for enhancing the representation. The layers are used with Quantum layers which improve the accuracy of registration. In GAN, the discriminator network is replaced with the encoder-decoder network U-net which improves the quality of the network by providing more semantic information. In addition to that, the layers of U-net are replaced with quantum layers in which encoding and transformation is applied based on non-linearity. Initially the input images are preprocessed to enhance the bone regions of the spine. After enhancement, the proposed inpainting is applied to register the image into 3D. The proposed approach is implemented in python software and the performance of 3D registration is evaluated with the performance metrics such as PSNR, SSIM etc. The proposed approach is compared to the existing registration techniques and it shows the efficiency of the GAN-Q-Unet approach. In future, it will be extended for multi domain environment to deal with different kinds of dataset.

Declaration of competing interest

The authors declare that they have no known competing financial interests or personal relationships that could have appeared to influence the work reported in this paper.

Data availability

Data will be made available on request.

References

[1] S. Agrawal, D.S. Sisodia, N.K. Nagwani, Neuro-fuzzy approach for reconstruction of 3-D spine model using 2-D spine images and human anatomy, in: Next Generation Computing Technologies on Computational Intelligence: 4th International Conference, NGCT 2018 vol. 4, Springer Singapore, Dehradun, India, 2019, pp. 102–115. November 21–22, 2018, Revised Selected Papers.

[2] Mingzheng Zhang, Wenxuan Chen, Shengru Wang, Siao Lei, Yuchen Liu, Jianguo Zhang, Fang Pu, Clinical validation of the differences between two-dimensional radiography and three-dimensional computed tomography image measurements of the spine in adolescent idiopathic scoliosis, World Neurosurgery 165 (2022) e689–e696.

[3] Zheye Chen, Lijun Guo, Rong Zhang, Zhongding Fang, Xiuchao He, Jianhua Wang, BX2S-Net: learning to reconstruct 3D spinal structures from bi-planar X-ray images, Comput. Biol. Med. (2023), 106615.

[4] Gueziri Houssem-Eddine, Drouin Simon, Charles XB. Yan, D. Louis Collins, Toward real-time rigid registration of intra-operative ultrasound with preoperative CT images for lumbar spinal fusion surgery, Int. J. Comput. Assist. Radiol. Surg. 14 (11) (2019) 1933–1943.

[5] Sampath Kumar, K.S. Hareesh, Soujanya Shetty, Validation of modified feature-based 3D modeling of scoliotic spine, Cogent Engineering 6 (1) (2019), 1623854.
[6] Yunliang Cai, Shaoju Wu, Xiaoyao Fan, Jonathan Olson, Linton Evans, Lollis Scott, Sohail K. Mirza, Keith D. Paulsen, Songbai Ji, A level-wise spine registration framework to account for large pose changes, in: International Journal of Computer Assisted Radiology and Surgery, vol. 16, Springer, 2021, pp. 943–953, 6.
[7] Liping Zhang, Lin Shi, Jack Chun-Yiu Cheng, Winnie Chiu-Wing Chu, Simon Chun-Ho Yu, LPAQR-Net: efficient vertebra segmentation from biplanar whole-spine radiographs, IEEE Journal of Biomedical and Health Informatics 25 (7) (2021) 2710–2721.
[8] T. De Silva, A. Uneri, X. Zhang, M. Ketcha, R. Han, N. Sheth, A. Martin, et al., Real-time, image-based slice-to-volume registration for ultrasound-guided spinal intervention, Phys. Med. Biol. 63 (21) (2018), 215016.
[9] Shan Liu, Bo Yang, Yang Wang, Jiawei Tian, Lirong Yin, Wenfeng Zheng, 2D/3D multimode medical image registration based on normalized cross-correlation, Appl. Sci. 12 (6) (2022) 2828.
[10] Roshan Ramakrishna Naik, H. Anitha, Shyamasunder N. Bhat, Nishanth Ampar, Raghuraj Kundangar, Realistic C-arm to pCT registration for vertebral localization in spine surgery: a hybrid 3D-2D registration framework for intraoperative vertebral pose estimation, Med. Biol. Eng. Comput. 60 (8) (2022) 2271–2289.
[11] Yunliang Cai, Shaoju Wu, Xiaoyao Fan, Jonathan Olson, Linton Evans, Lollis Scott, Sohail K. Mirza, Keith D. Paulsen, Songbai Ji, A level-wise spine registration framework to account for large pose changes, Int. J. Comput. Assist. Radiol. Surg. 16 (6) (2021) 943–953.
[12] Hooman Esfandiari, Carolyn Anglin, Pierre Guy, John Street, Weidert Simon, Antony J. Hodgson, A comparative analysis of intensity-based 2D–3D registration for intraoperative use in pedicle screw insertion surgeries, in: International Journal of Computer Assisted Radiology and Surgery, vol. 14, Springer, 2019, pp. 1725–1739, 10.
[13] Shengyu Zhao, Tingfung Lau, Ji Luo, I. Eric, Chao Chang, Yan Xu, Unsupervised 3D end-to-end medical image registration with volume tweening network, IEEE journal of biomedical and health informatics 24 (5) (2019) 1394–1404.
[14] Mathias Unberath, Cong Gao, Yicheng Hu, Max Judish, Russell H. Taylor, Mehran Armand, Robert Grupp, The impact of machine learning on 2d/3d registration for image-guided interventions: a systematic review and perspective, Frontiers in Robotics and AI 8 (2021), 716007.
[15] Wei Xia, Qingpeng Jin, Caifang Ni, Yanling Wang, Xin Gao, Thorax x-ray and CT interventional dataset for nonrigid 2D/3D image registration evaluation, Med. Phys. 45 (11) (2018) 5343–5351.
[16] Jun Liu, Gurpreet Singh, Subhi Al'Aref, Benjamin Lee, Olachi Oleru, James K. Min, Simon Dunham, Mert R. Sabuncu, Bobak Mosadegh, Image registration in medical robotics and intelligent systems: fundamentals and applications, Advanced Intelligent Systems 1 (6) (2019), 1900048.
[17] Payal Maken, Abhishek Gupta, 2D-to-3D: a review for computational 3D image reconstruction from x-ray images, Arch. Comput. Methods Eng. (2022) 1–30.
[18] Longwei Fang, Zuowei Wang, Zhiqiang Chen, Fengzeng Jian, Shuo Li, Huiguang He, 3D shape reconstruction of lumbar vertebra from two X-ray images and a CT model, IEEE/CAA Journal of Automatica Sinica 7 (4) (2019) 1124–1133.
[19] Veena Logithasan, Jason Wong, Marek Reformat, Edmond Lou, Using machine learning to automatically measure axial vertebral rotation on radiographs in adolescents with idiopathic scoliosis, Med. Eng. Phys. 107 (2022), 103848.
[20] Sunetra Banerjee, Juan Lyu, Zixun Huang, Frank HF. Leung, Timothy Lee, De Yang, Steven Su, Yongping Zheng, Sai Ho Ling, Ultrasound spine image segmentation using multi-scale feature fusion skip-inception u-net (siu-net), Biocybern. Biomed. Eng. 42 (1) (2022) 341–361.
[21] D. Yang, T.T.Y. Lee, K.K.L. Lai, Y.S. Wong, L.N. Wong, J.L. Yang, T.P. Lam, R. M. Castelein, J.C.Y. Cheng, Y.P. Zheng, A novel classification method for mild adolescent idiopathic scoliosis using 3D ultrasound imaging, Medicine in Novel Technology and Devices 11 (2021), 100075.
[22] Jiannan Zheng, Shun Miao, Z. Jane Wang, Rui Liao, Pairwise domain adaptation module for CNN-based 2-D/3-D registration, J. Med. Imag. 5 (2) (2018), 021204.
[23] Roman Schaffert, Jian Wang, Peter Fischer, Anja Borsdorf, Andreas Maier, Metric-driven learning of correspondence weighting for 2-D/3-D image registration, in: German Conference on Pattern Recognition, Springer, Cham, 2018, pp. 140–152.
[24] Xiaoxuan Zhang, Uneri Ali, Yixuan Huang, K. Craig, Timothy F. Witham Jones, Patrick A. Helm, Jeffrey H. Siewerdsen, Deformable 3D–2D Image Registration and Analysis of Global Spinal Alignment in Long-length Intraoperative Spine Imaging, Wiley online Library, Medical Physics, 2022.
[25] Weiwei Jiang, Qiaolin Xie, Yingyu Qin, Xiaojun Ye, Xiaoyan Wang, Yongping Zheng, A novel method for spine ultrasound and X-ray radiograph registration, Ultrasonics 133 (2023), 107018.
[26] Abir Dutta, Menaka Singh, Kathryn Kumar, Rodney Santiago, Ruchi Pathak Kaul, Sanganagouda Patil, Deepak M. Kalaskar, Accuracy of 3D printed spine models for pre-surgical planning of complex adolescent idiopathic scoliosis (AIS) in spinal surgeries: a case series, Annals of 3D Printed Medicine (2023), 100117.
[27] Mahsa Tajdari, Aishwarya Pawar, Hengyang Li, Farzam Tajdari, Ayesha Maqsood, Emmett Cleary, Sourav Saha, Yongjie Jessica Zhang, John F. Sarwark, Wing Kam Liu, Image-based modelling for adolescent idiopathic scoliosis: mechanistic machine learning analysis and prediction, Comput. Methods Appl. Mech. Eng. 374 (2021), 113590.
[28] Benjamin Aubert, Carlos Vazquez, Thierry Cresson, Stefan Parent, Jacques A. de Guise, Toward automated 3D spine reconstruction from biplanar radiographs using CNN for statistical spine model fitting, IEEE Trans. Med. Imag. 38 (12) (2019) 2796–2806.
[29] Shun Miao, Rui Liao, Agent-based methods for medical image registration, in: Deep Learning and Convolutional Neural Networks for Medical Imaging and Clinical Informatics, Springer, Cham, 2019, pp. 323–345.
[30] Nima Masoumi, Clyde J. Belasso, M. Omair Ahmad, Habib Benali, Yiming Xiao, Rivaz Hassan, Multimodal 3D ultrasound and CT in image-guided spinal surgery: public database and new registration algorithms, in: International Journal of Computer Assisted Radiology and Surgery, vol. 16, Springer, 2021, pp. 555–565, 4.
[31] Andrew Chan, Brendan Coutts, Eric Parent, Edmond Lou, Development and evaluation of CT-to-3D ultrasound image registration algorithm in vertebral phantoms for spine surgery, in: Annals of Biomedical Engineering, vol. 49, Springer, 2021, pp. 310–321, 1.
[32] Roman Schaffert, Jian Wang, Peter Fischer, Anja Borsdorf, Andreas Maier, Learning an attention model for robust 2-D/3-D registration using point-to-plane correspondences, IEEE Trans. Med. Imag. 39 (10) (2020) 3159–3174.
[33] Jun Soo Lee, Keewon Shin, Seung Min Ryu, Seong Gyu Jegal, Woojin Lee, Min A. Yoon, Gil-Sun Hong, Sanghyun Paik, Namkug Kim, Screening of adolescent idiopathic scoliosis using generative adversarial network (GAN) inversion method in chest radiographs, PLoS One 18 (5) (2023), e0285489.
[34] Woojin Lee, Keewon Shin, Junsoo Lee, Seung-Jin Yoo, Min A. Yoon, Yo Won Choi, Gil-Sun Hong, Namkug Kim, Sanghyun Paik, Diagnosis of scoliosis using chest radiographs with a semi-supervised generative adversarial network, Journal of the Korean Society of Radiology 83 (6) (2022).
[35] Zhongyi Han, Benzheng Wei, Ashley Mercado, Stephanie Leung, Shuo Li, Spine-GAN: semantic segmentation of multiple spinal structures, Med. Image Anal. 50 (2018) 23–35.
[36] Ching-Juei Yang, Cheng-Li Lin, Chien-Kuo Wang, Jing-Yao Wang, Chih-Chia Chen, Fong-Chin Su, Yin-Ju Lee, Chun-Chung Lui, Lee-Ren Yeh, Yu-Hua Dean Fang, Generative adversarial network (GAN) for automatic reconstruction of the 3D spine structure by using simulated Bi-planar X-ray images, Diagnostics 12 (5) (2022) 1121.
[37] Weiwei Jiang, Fang Mei, Qiaolin Xie, Novel automated spinal ultrasound segmentation approach for scoliosis visualization, Front. Physiol. 13 (2022), 1051808.
[38] Weiwei Jiang, Chaohao Yu, Xianting Chen, Yongping Zheng, Cong Bai, Ultrasound to X-ray synthesis generative attentional network (UXGAN) for adolescent idiopathic scoliosis, Ultrasonics 126 (2022), 106819.
[39] Olaf Ronneberger, Philipp Fischer, Thomas Brox, U-net: convolutional networks for biomedical image segmentation, in: Medical Image Computing and Computer-Assisted Intervention–MICCAI 2015: 18th International Conference, Springer International Publishing, Munich, Germany, 2015, pp. 234–241. October 5-9, 2015, Proceedings, Part III 18.
[40] Jonathan Long, Evan Shelhamer, Trevor Darrell, Fully convolutional networks for semantic segmentation, in: Proceedings of the IEEE Conference on Computer Vision and Pattern Recognition, 2015, pp. 3431–3440.
[41] Christa Zoufal, Aurélien Lucchi, Stefan Woerner, Variational quantum Boltzmann machines, Quantum Machine Intelligence 3 (2021) 1–15.
[42] http://spineweb.digitalimaginggroup.ca.
[43] Hooman Esfandiari, Weidert Simon, István Kövesházi, Carolyn Anglin, John Street, Antony J. Hodgson, Deep learning-based X-ray inpainting for improving spinal 2D-3D registration, in: The International Journal of Medical Robotics and Computer Assisted Surgery, vol. 17, Wiley online Library, 2021, p. e2228, 2.
[44] Ching-Juei Yang, Cheng-Li Lin, Chien-Kuo Wang, Jing-Yao Wang, Chih-Chia Chen, Fong-Chin Su, Yin-Ju Lee, Chun-Chung Lui, Lee-Ren Yeh, Yu-Hua Dean Fang, Generative adversarial network (GAN) for automatic reconstruction of the 3D spine structure by using simulated Bi-planar X-ray images, Diagnostics, mdpi.com 12 (5) (2022) 1121.
[45] Qi Sun, Rui Zhai, Fang Zuo, Yuhao Zhong, Yutao Zhang, A review of image inpainting automation based on deep learning, in: Journal of Physics: Conference Series, vol. 2203, IOP Publishing, 2022, 012037, 1.
[46] Jeroen Van Houtte, Emmanuel Audenaert, Guoyan Zheng, Sijbers Jan, Deep learning-based 2D/3D registration of an atlas to biplanar X-ray images, in: International Journal of Computer Assisted Radiology and Surgery, Springer, 2022, pp. 1–10.